Military Technical College
Kobry El-Kobbah,
Cairo, Egypt.

18th International Conference on Applied Mechanics and Mechanical Engineering.

INVESTIGATION OF THE INFLUENCE OF FLUIDICS INSERTION TECHNIQUE ON ARGON GAS ADDITIVES TO LPG ON THE TURBULENT LEAN PREMIXED FLAME CHARACTERISTICS FOR EV BURNER

S. Hassan[1], M. Elkady[2], H. Moneib[3], A. Omer[4], A. Emara[5], A. Attia[4] and A. Abdulnaim[6]

ABSTRACT

A series of experiments were done on a vertical EV burner with a constant coflow air of 873 L /min in order to investigate the impact of fluidics insertion technique on the temperature field and flame structure. The flow rates of fuel (LPG/ Ar) and air were measured using calibrated rotameters. The different volume ratios of the fuel constituents were admitted via three solenoid valves at the entry section of each stream prior to mixing and monitored using a lab view program. The axial temperature profiles at different operating conditions were measured using a bare (type S) thermocouple. Flame images were obtained, before and after fluidics insertion using a high resolution digital camera. The experimental program aims at identifying and analyzing the changes in flame characteristics (flame length, axial profiles of mean gas temperature, NOx concentration and overall combustion efficiency) resulting from the insertion of fluidics while considering different proportions of the fuel constituents. The results obtained indicate the following: it was noticed that in most cases of pure LPG only, and other mixtures of argon the images shows increase in both the length and luminosity of the flame as a result of higher degrees of swirl due to the fluidics insertion while the temperature profiles of the different flames were changed. It was indicated that NOx trend was decreased by 50% while the combustion efficiency was improved by 2.5%.

KEY WORDS

EV burner, Turbulent, Liquefied petroleum gas, Combustion efficiency, NOx.

---

[1] Egyptian Armed Forces and M. Sc. Student, Mechanical Power Eng. Dept., Faculty of Engineering, El-Azhar University, Cairo, Egypt.
[2] Professor, Mechanical Power Eng. Dept., Faculty of Engineering, El-Azhar University, Cairo, Egypt.
[3] Professor, Mechanical Power Eng. Dept., Faculty of Engineering-Mataria, Helwan University, Cairo, Egypt.
[4] Egyptian Armed Forces.
[5] Lecturer, Mechanical Power Eng. Dept., Faculty of Engineering-Mataria, Helwan University, Cairo, Egypt.
[6] Assist. Lecturer, Mechanical Power Eng. Dept., Faculty of Engineering-Mataria, Helwan Univ., Cairo, Egypt.

NOMENCLATURE

Ar Argon.
D Swirl stabilized burner diameter.
EV Environmental v shaped
LPG Liquefied petroleum gas.
T_{exh} Exhaust temperature.
x/D Radial location downstream of the burner.
y/D Axial location downstream of the burner.
Φ Equivalence ratio.
η_{Comb} Combustion efficiency.

INTRODUCTION

The word "Fluidics" is derived from two words "fluid" and "logic" and is used specifically to describe the technology of the control of fluid force components [1]. The fluidic oscillator is a device that generates an oscillating jet. When supplied with a pressurized fluid [2], See Fig. 1. Based on the operation principles, the fluidic oscillators are categorized as the feedback oscillator, the Karman vortex oscillator, and relaxation oscillator [3]. The Coanda effect has a major contribution to fluidic technology first described in the 1930's [1]. It describes the tendency for a jet of fluid (the fluid can be a liquid or a gas) issuing from a nozzle to adhere to the surface of the wall adjacent to it [4]. Fluidics is preferred to use in comparison to the valve arrangements. However, some tools that produce a pulsed jet through mechanical interruption or mechanical excitation of the normal or steady fluid flow would cause large energy losses, as well as mechanical wear and fatigue on the indispensable moving parts and seals [4]. Thereby, there is no need for maintenance requirements in the fluidics system which makes it highly appropriate for application in industrial gas turbines and has a long lifetime [5]. The modulation of dynamic behavior of the fluidic oscillator is performed by interactions among flow fluctuations in the inlet area, the growth of the recirculation flow, and the flow structure near step-walls and splitters [6]. Gregory adapted a fluidic oscillator as a dynamic calibration device for pressure instrumentation such as pressure-sensitive paint (PSP) [7].

A fluidic oscillator as shown in Fig. 1, includes an oscillator body which have two attachment walls defining an oscillating chamber there between, an inlet duct extended to the oscillating chamber for guiding a flow of fluid entering into the oscillating chamber. It also includes, two outlet ducts communicatively extended from the oscillating chamber for guiding the flow of fluid exiting from the oscillating chamber, and two feedback channels communicating with the oscillating chamber. Each attachment wall has an upstream portion and a downstream portion integrally extended therefrom as a step shouldering manner to form a modulating shoulder. This shoulder is used for modulating an oscillation of the flow within the oscillation chamber for stabilizing the flow of the fluid to pass through the oscillator body. A flow splitter divides the exit duct after the control throat into two equal portions. For the application of the fluidic oscillator in a combustion system as shown in Fig. 2. Paschereit [8] inserted the fluidics oscillator for controlling the actuation frequency and the amplitude.

The investigation of injected mixture of Acetylene/Argon gases to the liquefied petroleum gas (LPG) in different concentrations on coflowing jet turbulent lean premixed flames is remarkable. Argon (Ar) is considered the third most common gas in the Earth's atmosphere. About 700,000 tons of Ar are produced worldwide every year. Ar occurs naturally in air, and is readily obtained as a byproduct of cryogenic air separation in the production of O_2 and N_2. Ar has been already used in internal combustion engine. It has an effect in combustion increasing efficiency [9, 10].

There are two types of additives that may be added to the hydrocarbon fuel either to decrease soot emissions or to increase it. These are explained as follows:

(i) Additives that decrease soot emission: These additives include inert gases such as Ar, He and N_2, hydrogen, CO_2, H2O and SO_2. Inert gases generally decrease the tendency to soot formation.

(ii) Additives that increase Soot formation: These additives include:

- Halogens (particularly bromine): These act by catalyzing radical recombination, thus neutralizing excess OH radicals which could otherwise oxidize soot or soot precursors.
- Oxygen: The effect of oxygen addition to the fuel is complicated. Some writers found that O_2 acts as soot promoters while others found it to be a soot inhibitor; for example:
  (a) In ethylene flames, small addition of O_2 results in noticeable increased soot emissions. The presence of O_2 accelerates the pyrolysis polymerization reactions occurring in the ethylene; (Wright et al 1961) [11] This is also confirmed by the studies on ethane, butane, propane, propylene and benzene diffusion flames; (Schug K.P et al 1980) [12].
  (b) In propane, butane and propylene, O_2 suppresses soot emissions; (Gay et al 1961) [13].

EXPERIMENTAL SET UP, FACILITIES AND EXPERIMENT PERFORMANCE

The present work aims to study the effect of fluidics insertion technique on Acetylene/Argon gas additives to the liquefied petroleum gas (LPG) on the turbulent lean premixed flame characteristics for EV Burner. The measurement system can be configured to measure some or all of the flame parameters depending upon the application requirements. The measurement results can be used to predict and diagnose combustion phenomenon. The assembly and schematic diagram of system set-up is shown in Fig. 3 In addition, Fig. 3 shows the items of the test rig and measuring instruments.

The lean premixed coflowing jet turbulent flames were established on a flat EV burner with an air coflow injected upstream the flow (Figure 4) [14].The manufacturing process for the EV burner components with the fluidics and its mechanism shown in Fig. 4 was done on CNC milling-turning machine due to its high degree of precision and accuracy. For the EV burner with the inserted fluidics; Figure 4 shows the modifications done in the EV burner after being manufactured in order to adapt the burner for cold and hot flow Conditions. These modifications include:

1- A mixer of gases fixed at the top of fuel pipe with three inputs for mixing of different gases.
2- A burner flange for vertical suspension of EV burner in the test rig.

3- A secondary cylindrical air tube threaded from one side with the burner flange while its other side is closed by a flange with four inputs of air to take pure pressurized air from the compressor 12 bar and this four inputs with circular outputs for swirling the air coming from the compressors in order to improve mixing of gases with air and for combustion enhancement [15].
4- A stainless steel pipe of diameter 21.3 mm was fitted inside the fuel pipe of EV Burner to separate the fluidics line from the main fuel line.
5- A threaded fluidics mechanisms also was fixed on the upper end of the fluidics with two inputs including two supports which facilitate the easy motion for the fluidics inside the whole cone length of EV Burner [16, 17]. The fluidics was manufactured also on CNC milling-turning machine due to its high degree of precision and accuracy according to the model (FX1) developed by Emara [14].

The combustion flames were in room atmospheric conditions with room disturbances controlled by surrounding. A cylindrical silica glass was put upward the burner rim with 30 cm length and 1cm thickness in order to treat such flames as free jet turbulent lean premixed flames and through this silica transparent glass we can visualize flame and taking a lot of digital images at different conditions while at the same time keeping the flame with confined characteristics. Also, the silica glass was replaced by a stainless steel cylindrical tube (Combustor) of 30 cm length and with 14 vertical holes of 1cm diameter on its left side for inserting thermocouple through these holes for inflames radial and axial measurements. The instrumentation of the burner including the PC were connected in such a way to provide safe ignition conditions. The control card was powered by a 5V DC power supply. Air compressors 12 bar regulated to 1bar gauge pressure supply air mass flow rates. Wide range of flow rates, mostly dry, is measured by calibrated standard flow rotameters (model KI-USA) and is controlled by precision needle valves. In order to admit accurate flow rates of both the gaseous fuel and the coflowing air, four flow supply and metering systems for LPG, Argon, Acetylene and air are used. In this work fuel and air flow rates measurements are made using rotameters manufactured by Dwyer Instruments Inc. Since all the rotameters used are calibrated for air at standard pressure and temperature, the flow-rate readings taken were corrected according to the calibration equations supplied by the manufacturer for the flow pressure. Five solenoid valves were used and controlled by Lab View program.

The turbulent lean premixed flame, axial temperature profile were measured using a shielded-aspirated thermocouple platinum/ Platinum -10% Rhodium (type S) with maximum temperature of 1800 ℃, ≤ 250μm diameter, ±0.5% uncertainty limit and response time of 0.3 second. A digital muffle furnace is incorporated for the calibration and the results showed a difference of 1-2 %.The probe offers the minimal possible disturbances. The output voltage from the thermocouple is acquired using the Omega interface program thermocouple reader and PC. Radiation error is due to radiant heat transfer from the temperature sensor to its surroundings while conduction error is due to time lag needed to heat the thermocouple bead. The magnitude of the thermocouple errors can be reduced by taking several relatively simple steps: (i) use as small thermocouple bead as possible. (ii) use new shiny thermocouples. The low emissivity minimizes radiational heating. Using a shielded-aspirated thermocouple reduces the error in the average trace. Highest accuracy is attained when using small diameter shielded-aspirated thermocouples [18-20].

Flame images were taken using Canon 6D 20.2MP full frame camera with high resolution Lens 70 – 200 F2.8L IS II USM with sensor having a speed of up to 3.7 fps was used to obtain visual images of the flames under different operating conditions. All shots were taken in the night vision mode with shutter speed of 1/60 s to express the average flame shape. The visual flame length was measured by comparing the flame length in the photo by a reference length scale. Injecting of diluents affects the turbulent lean premixed process, flame length and temperature distribution through the flame.

Experiment Performance

Before performing the experiment, the system must be completely free of leaks to prevent errors in flow rate measurements and maintain a safe working environment. The flow rate of the coflowing air was firstly adjusted which kept constant through the whole experiments at 873 Lit/min then the rate of LPG and at last the rate of the diluents. A series of experiments were performed as presented in Table 1. The mixing of gases was based on the volume flow rate of gases injected to the burner. The choice of the different cases was based on flame stability. The air flow rate was kept constant as mentioned before in all cases. The fuel used was LPG with flow rate from 16 up to 32 L/min, Ar flow rate from 2.8up to 12 L/min. The total mixture flow rate (LPG + Ar) didn't exceed 40 L/ min in order to prevent the flame instabilities.

In cases (1, 2) without fluidics and FX1(1,2) with fluidics representing the base line only LPG and air were used. In the cases (2A,2B,2C),(3A,3B,3C,3D), (4A,4B,4C,4D) without fluidics, a Sets of experiments were conducted through which Argon is progressively added (from 10 % up to 30 %) with a corresponding reduction of LPG (from 90% to 70%) respectively . In each case the total volume flow rate is increased progressively from 28 Lit / min to 40 Lit / min with an incremental increase of 4 Lit / min. These permit the identification of:

(i) The effects of varying the diluent concentration on the flame characteristics at varying total flow rates of the fuel mixture via comparing the data being obtained in cases (2A,3A, 4A) - (2B, 3B, 4B) - (2C,3C, 4C) (3D, 4D); (see Table 1).
(ii) The effects of varying the total mixture flow rate on flame characteristics at a given diluent concentration via comparing the data being obtained in cases (2A, 2B, 2C) - (3A, 3B,….to 3D), (4A,4B,….to 4D) ;(see Table 1) .

In the cases (2A, 3A, 4A) FX1 with fluidics, a Sets of experiments were conducted through which Argon is progressively added as previously (from 10 % up to 30 %) with a corresponding reduction of LPG (from 90% to 70%). In each case the total volume flow rate is increased progressively from 28.6 Lit /min to 33.8 Lit /min while keeping LPG flow rate at 26 Lit /min for focusing at this case after inserting fluidics and comparing it with cases (2A and 3B) in Table 1 free from fluidics .These permit the identification of:

(i) The effects of varying the diluent concentration on the flame characteristics at varying total flow rates of the fuel mixture via comparing the data being obtained, see Table 1 cases : (2A - 3A) free from fluidics , with the data obtained, see Table 1 cases : (2A - 3A) FX1 after inserting fluidics .
(ii) The effects of varying the total mixture flow rate on flame characteristics at a given diluent concentration via comparing the data being obtained, see

Table 1 cases : (2A and 3B) free from fluidics , with the data obtained see Table 1 cases : (2A and 3A) FX1 after inserting fluidics .

In order to detect the temperature distribution through the flame, the temperature was measured in axial directions. The reference point of all measurements was at "0" corresponding to the center of the burner (Figure 5). All these runs in Table 1 were performed for detecting the trends of different parameters like, NOx and combustion efficiency, axial temperature distribution and digital images for the different selective cases required to investigate the influence of fluidics insertion technique on Argon gas additives to LPG on the turbulent lean premixed flame characteristics for EV Burner. In the following, the results obtained in the eighteen investigated cases and their discussions are presented.

Cases from (1 to 4A FX1) which appear in Table 1 Include temperature measurements in axial distances (y/D) from (0 to 1) at the center of the flame, also digital images was detected for cases (1,1FX1), (2A,2B,2C), (3A,3B,3C,3D), (4A,4B,4C,4D) , (2A,3A,4A)FX1 , and the influence of fluidics insertion technique in EV Burner on combustion efficiency, NOx, axial temperature distribution were detected for the mentioned cases.

RESULTS AND DISCUSSIONS

In the following, the results obtained in the eighteen investigated cases listed Table 1 and their discussions are presented.

Cases (1, 2), FX1 (1, 2)

Figure 6 shows two visual images of the pure LPG turbulent lean premixed flames at volume flow rates 26 L/min where Φ = 0.82, [Case1FX1 with fluidics , Case1 free from fluidics]. It was intended to take these two visual images for the flame at the same boundary conditions for precise evaluation of the flame characteristics after fluidics insertion technique. Careful examinations of the flame images in Fig. 6 (boundaries, colors, contours) indicate the following findings:

The increase in both length and luminosity as a result of high degrees of swirl is appeared in Fig. 6. The flame view in Case 1 FX1 on the left flame image shows high degree of swirl due to the fluidics insertion than the right flame image free from fluidics Case 1. Figure 7 shows the influence of fluidics insertion on the axial distribution of mean flame temperature at volumetric flow rate of pure LPG =26 L/min, where Φ = 0.8. It was indicated that the maximum mean flame temperature was 1091.2℃ at Case 1 free from fluidics and also 1040℃ at Case 1FX1 with fluidics all the above temperatures were in an axial distance of y/D = 0.24 , from the burner rim . This indicates that the temperature profiles of pure LPG flames were changed after fluidics insertion. Figures 8, 9 show the influence of fluidics insertion on NOx reduction and combustion efficiency improvement at volumetric flow rate of pure LPG = 26 L/min, where Φ = 0.8, Cases (1, 2 , 1FX1,2FX1) It was indicated that the NOx trends was decreased by 54% ,while the combustion efficiency improved by 4.5% after inserting fluidics FX1 in EV Burner 2 slots .

Cases (2A to 2C)

The temperature of the flame increased along the center of the flame in axial direction the maximum. flame temperature reaches about 1051.4 ℃, which was in an axial distance of y/D = 0.24 about 2cm apart from the burner rim, see Fig. 10 case 2A.The temperature distribution is presented in Fig. 11 which shows axial measurements in definite points according to flame zones with radial variation. The temperature increased in the direction of flame boundaries to the maximum temperature of 1270,1033 , 880 ℃ at Y (axial distance) = 2, 4, and 6cm from the burner dump plane respectively, also the other radial variations at Y (axial distance) from 8cm up to 18cm were measured and appear in Fig. 11 case 2A .

Cases (3A to 3D)

The fuel was modified by using a mixture of 80% LPG and 20% Argon. As in the previous runs, the smoke number was detected in Fig. 12 which appears that it was decreased to smoke number zero due to argon addition; the radial variation of temperature distribution was measured in definite axial positions as shown in Fig. 13, run 3B. The temperature increased in the direction of flame boundaries to the maximum temperature of 1275,1051 , 895 ℃ at Y (axial distance) = 2, 4, and 6cm from the burner dump plane respectively, also the other radial variations at Y (axial distance) from 8cm up to 18cm were measured and appear in Fig. 13 also. The temperature of the flame increased along the center of the flame in axial direction; the maximum flame temperature reaches about 1039 ℃, which was in an axial distance of y/D = 0.24 about 2cm apart from the burner rim see Fig. 14 .

Cases (1 and 3B)

Figure 15 shows the influence of argon addition on mean flame temperature along axial distance at Φ = [0.8], Run [1 pure LPG, 3B mixture of LPG, Ar] It is obvious that the trend of mean flame temperature along the axial distance of EV burner was decreasing after addition of argon percentage on pure LPG. The maximum mean flame temperature was 1091.2℃ in case 1 of pure LPG and decreased to be 1020.2℃, , in case 3B of mixture of LPG & Argon .

Cases (2A to 2C & 3A to 3C)

Figure 16 panels a, b shows the variations of the exhaust temperature, NOx with the input volume flow rate of LPG and Ar flames runs (2A to 2C & 3A to 3C) which indicates the decrease of the exhaust temperature, NOx ranges with the increasing of the addition of Argon percentage to the pure LPG and this is due to the temperature reductions resulting from the higher thermal capacity of Argon (diluent) and the lower heating value of the fuel mixture.

Cases (2A, 2B, 2C),(3A,3B,3C,3D), (4A,4B,4C,4D)

Figure 17 shows the relation between combustion efficiency and the flow rates of LPG and Argon flames, runs (2A to 2C, 3A to 3D, 4A to 4C). It was noticed that the combustion efficiency trend decreasing by increasing the Argon % addition while decreasing LPG percentage. Figure 18 panels a, b, c show the variations in the digital flame images associated with the progressive addition (10% to 30%) of Argon

(diluent) to the base fuel (LPG) at different fuel flow rates for any particular mixture; (see also Table (1) .The following observations and interpretation may be outlined as follows:

1- Referring to Fig. 18 panels a, b, c it is clearly seen that: The progressive increases of Argon at any particular fuel flow rate cause a decrease in the visible flame length. This visible length is lower than that in the pure LPG cases at the same input volumetric fuel flow rate. Also at any particular degree of Argon dilution, the visible flame length does not linearly increase with the progressive increase of the fuel mixture low rate; a typical characteristic of turbulent premixed flame. But the stream lines of the flame increases linearly with the progressive increase of the fuel mixture flow rate.
2- The degree of flame luminosity decreases with the increase of Argon dilution at any particular fuel flow rate; a fact which reflects an overall decrease of the local flame temperatures as a reason of (i) the lower degree of mixing between reactants and oxidant, (ii) the temperature reductions resulting from the higher thermal capacity of argon (diluent) and (iii) the lower heating value of the fuel mixture.
3- With the progressive increase of Argon flow rate, Figure 18 Indicates that the flame length (Lf) increased in all runs.

Cases (2A, 3A, 4A) FX1

Panels (a-b) of Fig. 19 show the variations in the digital flame images associated with the progressive addition (10% to 30%) of Argon (diluent) to the base fuel (LPG) at different fuel flow rate for any particular mixture; with or without Fluidics (see also Table 1). The following observations and explanations may be drawn;

1- Referring to Fig. (19), it is clearly seen that; at any particular degree of Argon dilution, the visible flame length not linearly increases with the progressive increase of the fuel mixture flow rate; a typical characteristic of turbulent premixed flame. However, the stream lines of the flame increases linearly with the progressive increase of the fuel mixture flow rate and this clearly appears in panels (a-b)

2- The degree of flame luminosity decreases with the increase of Argon dilution at any particular fuel flow rate; a fact which reflects an overall decrease of the local flame temperatures as a reason of (i) the lower degree of mixing between reactants and oxidant, (ii) the temperature reductions resulting from the higher thermal capacity of argon (diluent) and (iii) the lower heating value of the fuel mixture also this appears in panels (a-b)

3- With the progressive increase of Argon flow rate, (Figure 19 panels a-b) the flame length (Lf) apparently increases in all runs .

CONCLUSIONS

The investigation of injected mixtures of air, LPG, Argon in different concentrations on a coflowing jet turbulent lean premixed flames and their analysis for the mentioned 18 Runs in Table 1 of the experimental program lead to the following conclusions:

Concerning the analysis of the variations in the thermal structures:

- In case of pure LPG the maximum axial flame temperature at Φ = 0.8, 1 was 1091℃, 1191℃ respectively. By Argon addition to LPG the maximum axial flame temperature at Φ = 0.8 was 1039℃.
- The radial distributions of mean gas temperature along the flame length clearly indicate that the maximum temperature was at the flame center (visible flame) in all cases. While the temperature started to decrease gradually until reach the flame outer boundary (invisible flame) attached to the combustor wall.

Concerning the analysis of the variations in smoke number and soot volume fraction:

- In case of pure LPG only the smoke number is = 1, SVF ranges = 0.05 - 0.09 ppm. By Argon addition to LPG the smoke number indicator decreased to zero, SVF ranges = 0 – 0.049 ppm.

Concerning the analysis of the variations in exhaust temperature:

- In case of pure LPG the exhaust temperature increases by the increasing the fuel flow rate of LPG. By Argon addition to LPG the exhaust temperature trends show a decrease in its ranges due to the temperature reductions resulting from the higher thermal capacity of Argon (diluent) and the lower heating value of the fuel mixture.

Concerning the analysis of NOx , combustion efficiency:

- In case of pure LPG the NOx emissions were increasing by increasing of pure LPG flow rates. While combustion efficiency maximum value around 56.14% at Φ = 1. By Argon addition to LPG It was noticed that the NOx trend and combustion efficiency decreased by increasing the Ar % addition while decreasing LPG %.

Concerning the fluidics insertion on , images , axial temperature distribution, NOx, combustion efficiency:

- Visual analysis of the flame structure; whereby digital images , the variations in visual flame length along the different flames are compared and analyzed when fluidics being inserted in the EV burner or not .
  - In the most cases of pure LPG only, LPG + Argon the images shows increase in both the length and luminosity of the flame as a result of higher degrees of swirl due to the fluidics insertion.
- In case of LPG + Argon the influence of fluidics insertion appears clearly on the axial distribution of mean flame temperature at volumetric flow rate of mixture of LPG with Argon (diluent) added by percentage 10-20% while LPG =26 Lit / min, where Φ = (0.82). It was indicated that the maximum flame temperature was 1151℃ , 1107℃ free from fluidics while these temperatures was decreased to 1036℃ , 1012 ℃ when fluidics was inserted .
- In case of pure LPG only at V_{LPG} = 26 Lit / min, where Φ = 0.8, It was indicated that the NOx trends was decreased by 54%, while the combustion efficiency improved by 4.5% after inserting fluidics.
- In case of LPG + Argon, when Argon (diluent) added with percentages 10-20% while LPG = 26 Lit / min, where Φ = 0.82, it was indicated that the NOx

trends was decreased by 50% ,while the combustion efficiency improved by 2.5% after inserting fluidics FX1.

REFRENCES

[1] Giles B. D., "Fluidics, the Coanda Effect, and Some Orographic Winds", Springer- Verlag, 1977.

[2] Gregory J. W., Sakaue H. and Sullivan J. P., "Fluidic oscillator as a dynamic calibration tool", AIAA 2002-2701, St. Louis, Missouri, 2002.

[3] Yang J., Lin W., Tsai K. and Huang K., "Fluidic Oscillator",US 6,860,157 B1, 2005.

[4] Griffin W.A. and Almeida S.M.," Pulsation nozzle, for self- excited oscillation of drilling fluid jet stream ", US Patent 5495903, 1996.

[5] Follows P., Williams M. and Murray P., "Applications of Power Fluidics technology in nuclear waste processing plants", WM'05 conference, Tucson, 2005.

[6] Yang J., Chen C., Tasi K., Lin W. and Sheen H., "A novel Fluidic oscillator incorporating step- shaped attachment walls", Elsevier, 2006.

[7] Gregory J.W., Sakaue H. and Sullivan J.P., "Fluidic oscillator as a Dynamic calibration tool", AIAA 2002-2701, St. Louis, Missouri, 2002.

[8] Guyot D. and Paschereit C. O., "Active control of combustion Instability using symmetric and asymmetric premixed fuel modulation" ASME paper GT2007-27342, Montreal, Canada, 2007.

[9] Li W. F, Liu Z. C., Tian J., Wang. Z. S and Xu Y. , "Effects of argon dilution on the thermal efficiency and exhaust emissions of a NG engine ", International Journal of Automotive Technology , Volume 16, Issue 5, pp 721-731, 2015.

[10] Periodic Table of Elements: Argon — Ar. (2008). http://www. Environmental chemistry.com.

[11] Wright J. R., (1961),"Effect of Oxygen on Carbon-Forming Tendencies of Diffusion Flames", Fuel, Vol. 53, pp. 232-235.

[12] Schug K.P., Manheirner-Timmat Y., Yaccarino P. and Glassman,I.,"Sooting Behavior of Gaseous Hydrocarbon Diffusion Flames and the influence of Additives", Combust. Sci. and Tech., 22, 235-250, (1980).

[13] Gay N. R., Agnew J. T., Witzell O. W. and Karabell C. E., "Thermochemical Equilibrium in Hydrocarbon-Oxygen Reactions Involving Polyatomic Forms of Carbon", Combustion and Flame, Vol. 5, pp. 257-272 (1961).

[14] Emara A., "Interaction of flow field and combustion characteristics in a Swirl stabilized burner", Ph.D. thesis, Technical university, Berlin, Germany, 2011.

[15] Hassan S., Emara A. and Elkady M.,"Evaluation of EV Burner Performance through Pilot Injection Technology: A Review ", IJESC, ISSN 2321 3361, 2016.

[16] Hassan S., Emara A. and Elkady M., "Enhancement of Propulsion Performance through Fluidcs insertion Technology in EV burner:A Review", IJSER, ISSN 2229-5518, 2016.

[17] Hassan S., Emara A. and Elkady M., "An Investigation of Argon Gas Additives to LPG on the Turbulent Lean Premixed Flame Characteristics For EV Burner", IJSER, ISSN 2250-1371, ©2017.

[18] Shannon K. S., Butler B.W, "A review of error associated with thermocouple temperature measurement in fire environments", USDA Forest Service, Fire Sciences Laboratory, Rocky Mountain Research Station Missoula, Montana (2002).

[19] Shaddix C. R., "Practical aspects of correcting thermocouple measurements for radiation loss." Fall Meeting of Western States Section/The Combustion Institute (1998).
[20] Jones J.C., (1995) "On the use of metal sheathed thermocouples in a hot gas layer originating from a room fire". Journal of Fire Science, 13, 257-260.

Figures and Table:

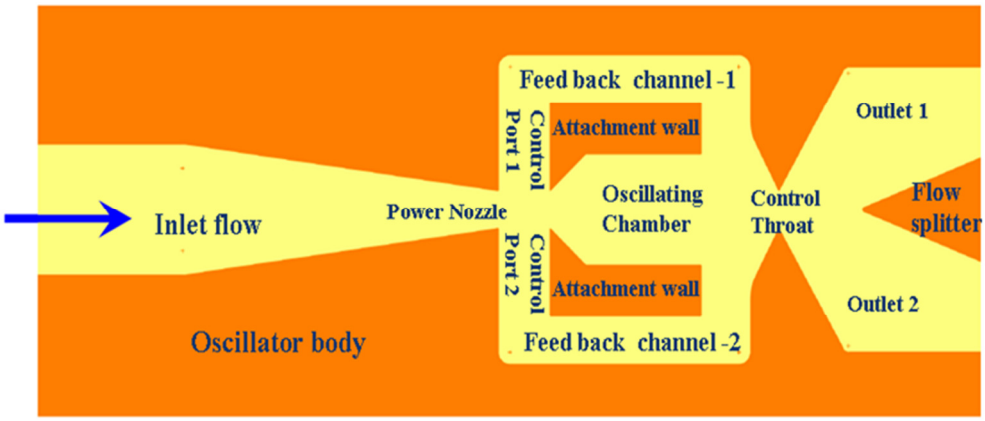

Fig.1. Schematic diagram of the fluidic oscillator.

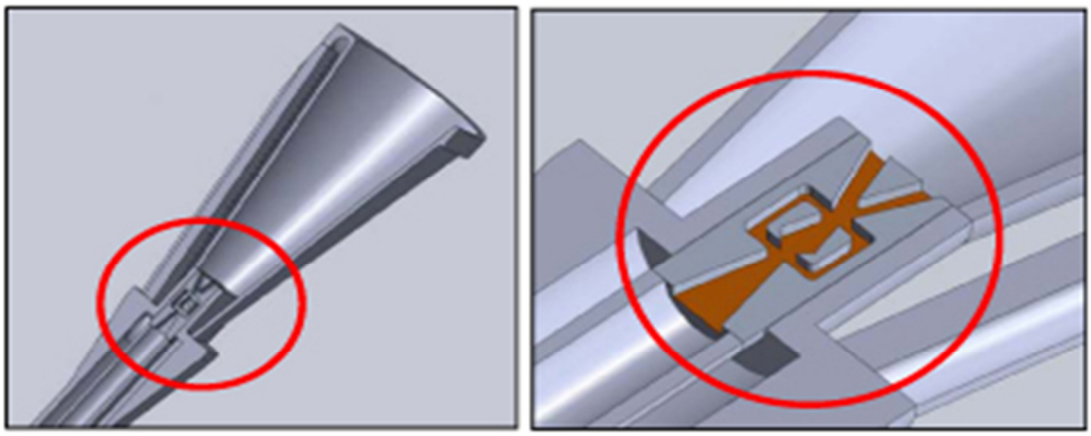

Fig.2. Swirl burner with fluidic oscillator integrated into the pilot fuel lance and also into the premix fuel supply .

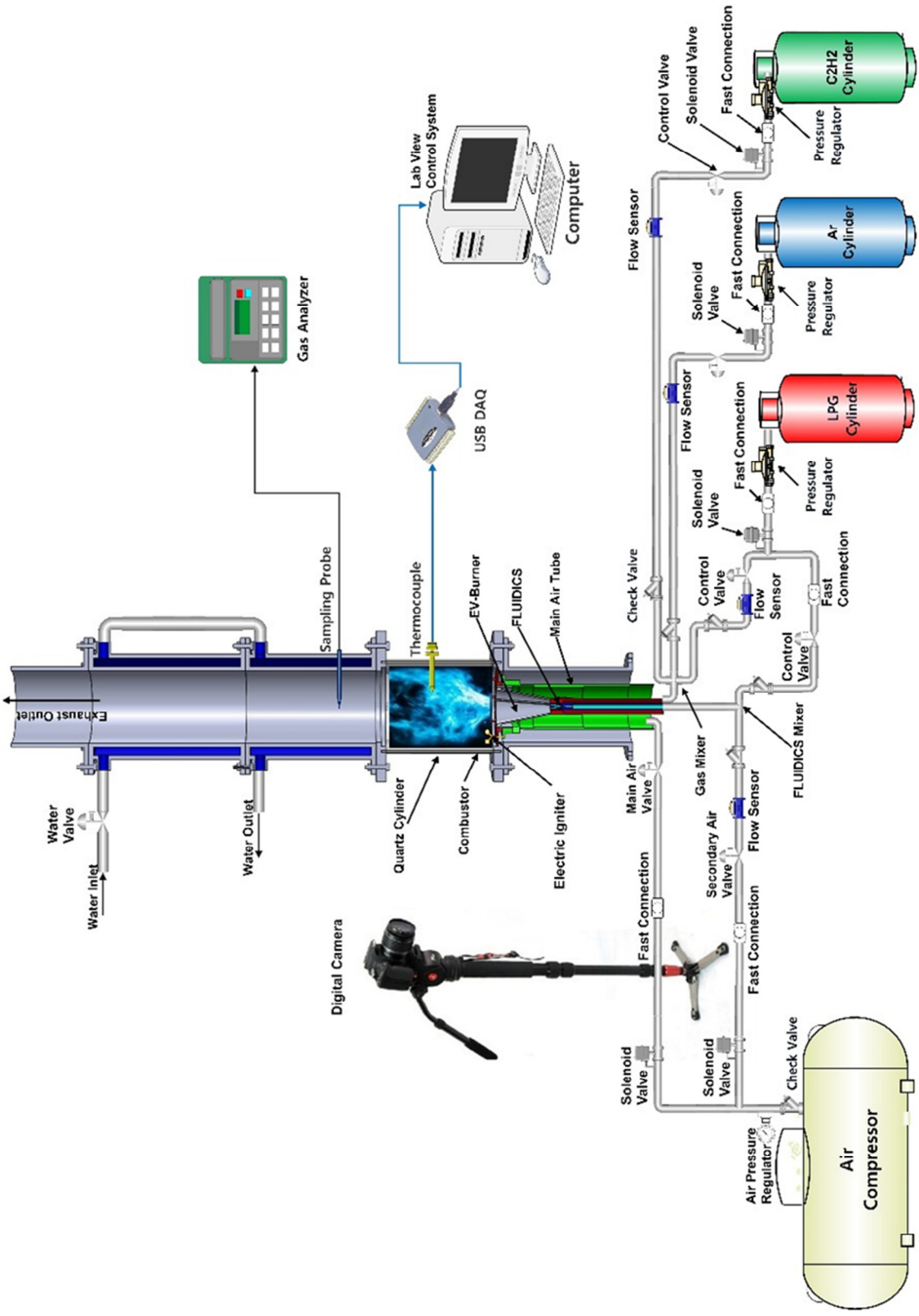

Fig. 3. Schematic diagram of EV Burner test rig including the fluidics mechanism**.**

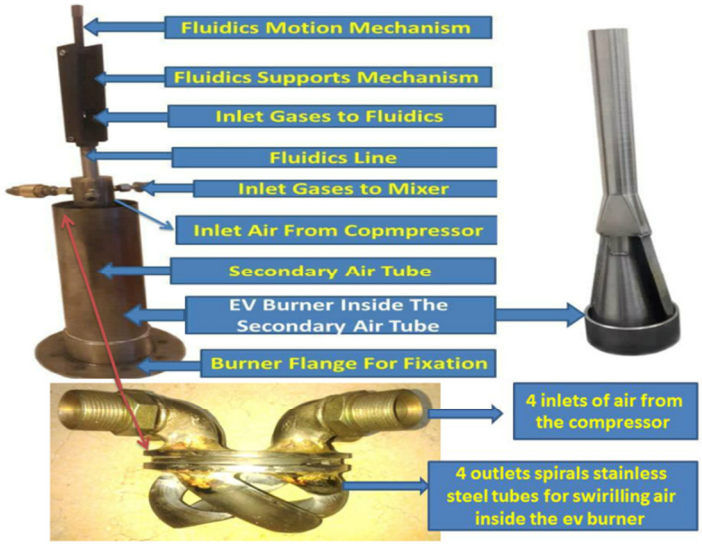

Fig. 4. Fuel, Air connections in EV Burner and fluidics mechanism.

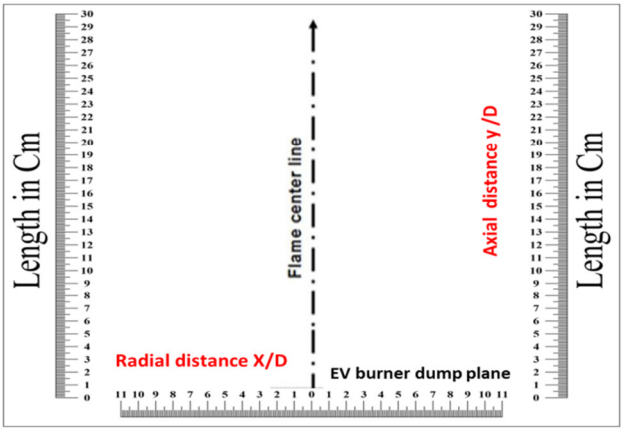

Fig. 5. Schematic representation of axial, radial directions.

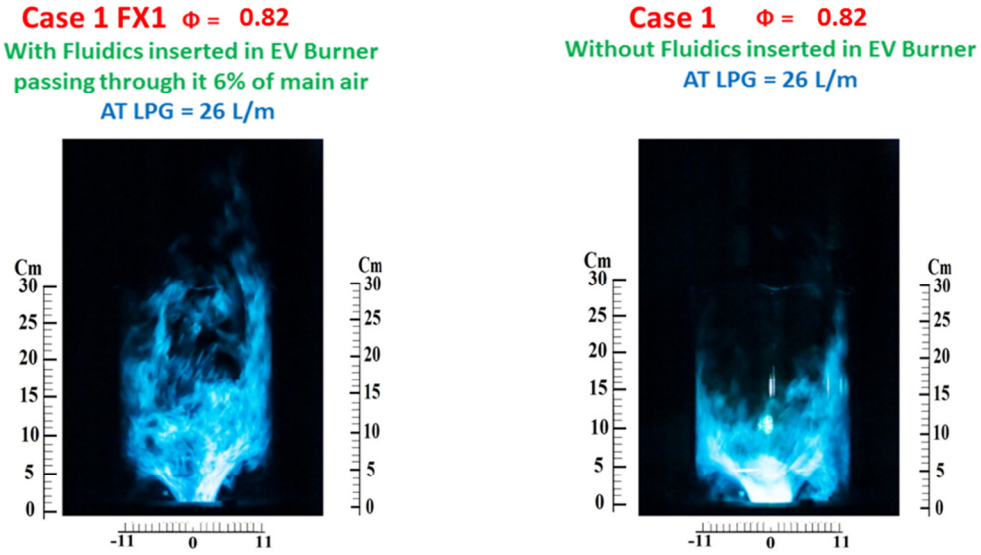

Fig. 6. Visual images of the pure LPG turbulent lean premixed flames at volume flow rates 26 L/min [Case 1FX1 with fluidics , Case 1 free from fluidics] .

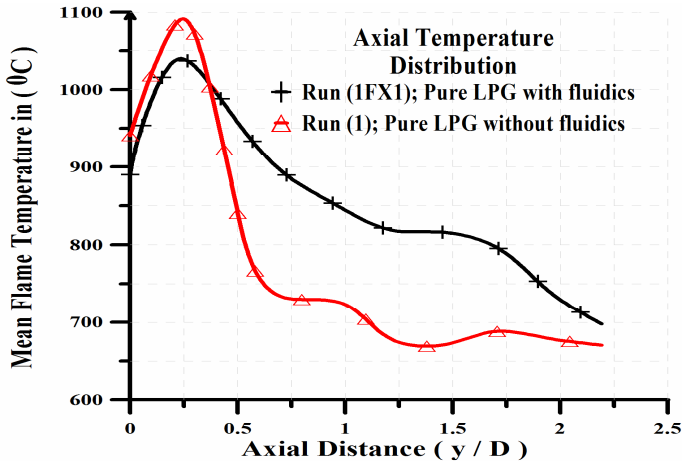

Fig. 7. Influence of fluidics insertion on axial distribution of mean flame temperature at flow rate of pure LPG.

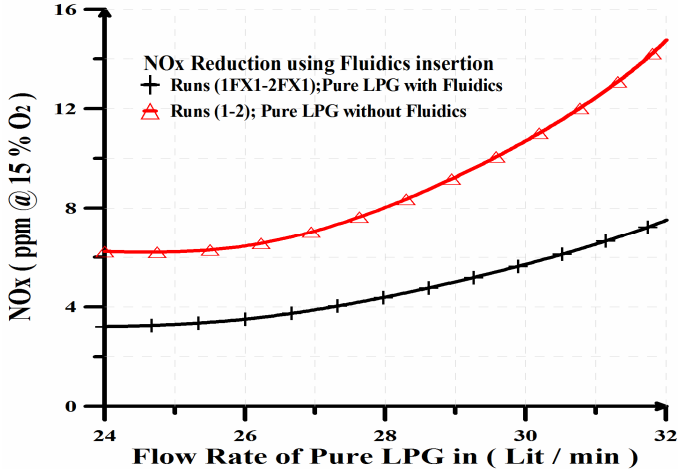

Fig. 8 . Influence of fluidics insertion on NOx reduction for a flow rates of pure of LPG, cases [1, 2, 1 FX1, 2 FX1].

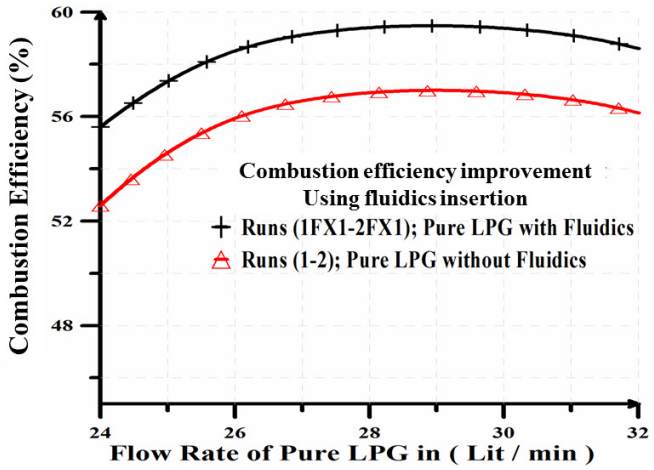

Fig. 9. Influence of fluidics insertion on combustion efficiency for a flow rates of pure LPG,[1, 2, 1 FX1,2 FX2].

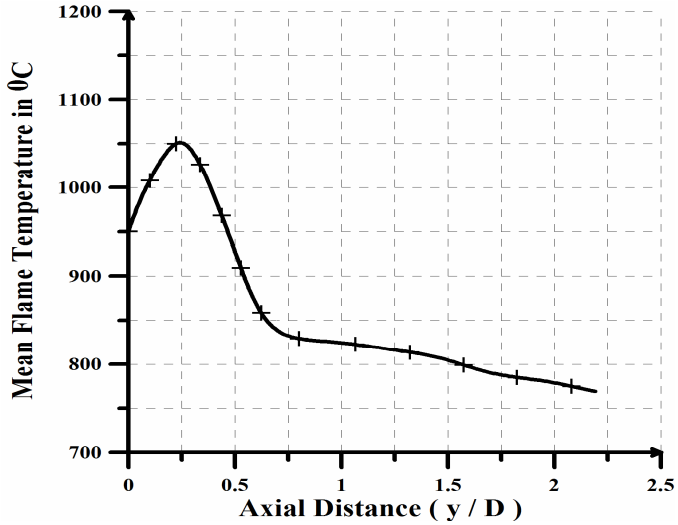

Fig. 10. Temperature distribution through the center of the flame in run 2A.

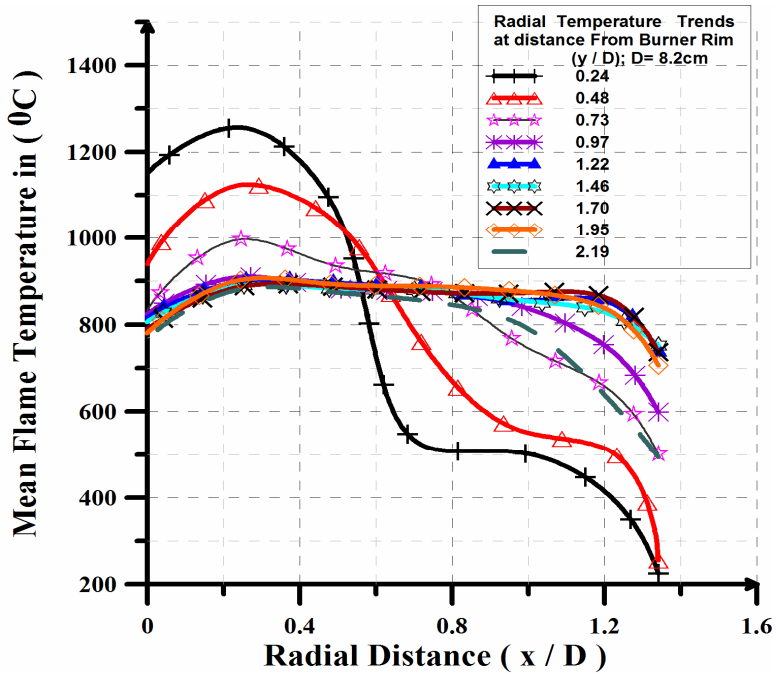

Fig. 11. Temperature distribution across the flame in run 2A. Φ = 0.79.

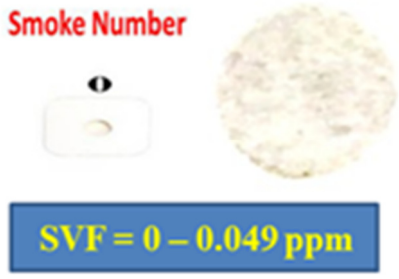

Fig. 12. Smoke number at run 3B.

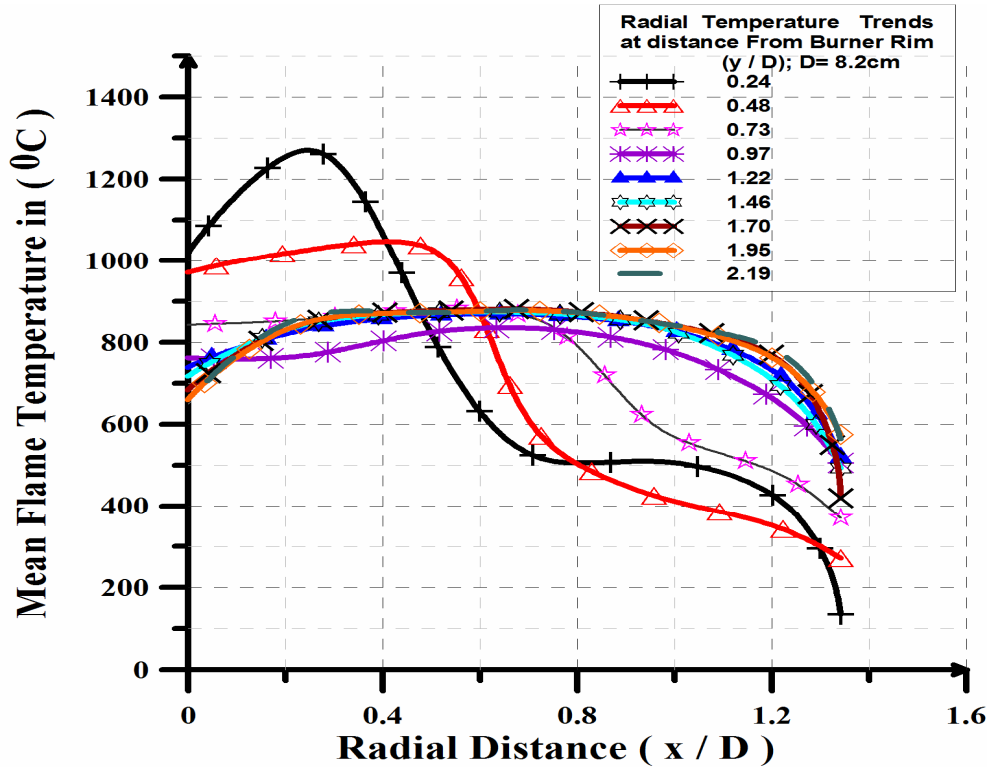

Fig. 13. Temperature distribution across the flame in run 3B.

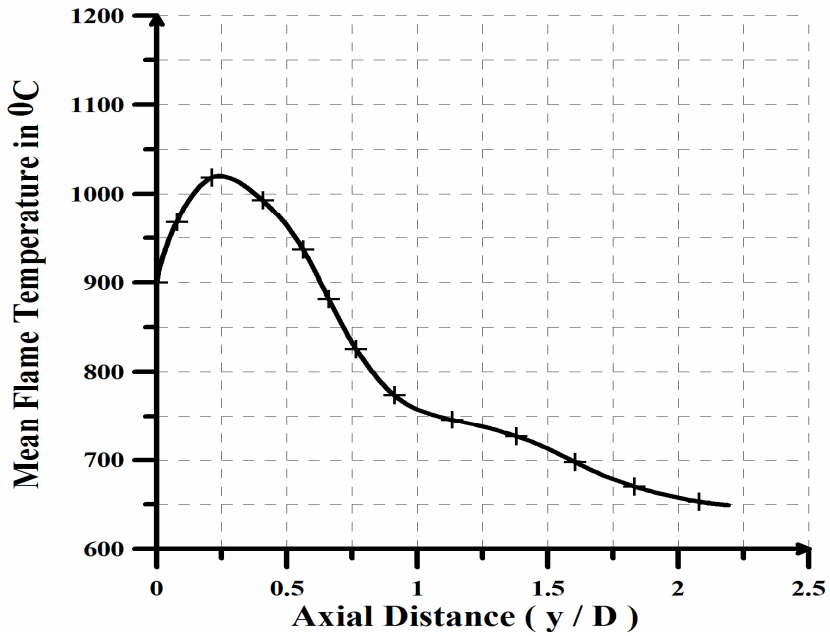

Fig. 14. Temperature distribution through the center of the flame in run 3B.

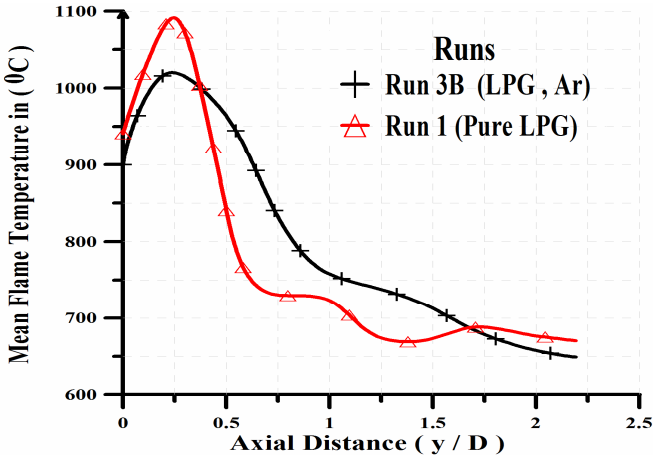

Fig. 15. Influence of Argon addition on mean flame temperature along axial distance at Φ = [0.8] , Run [1C – 3B] .

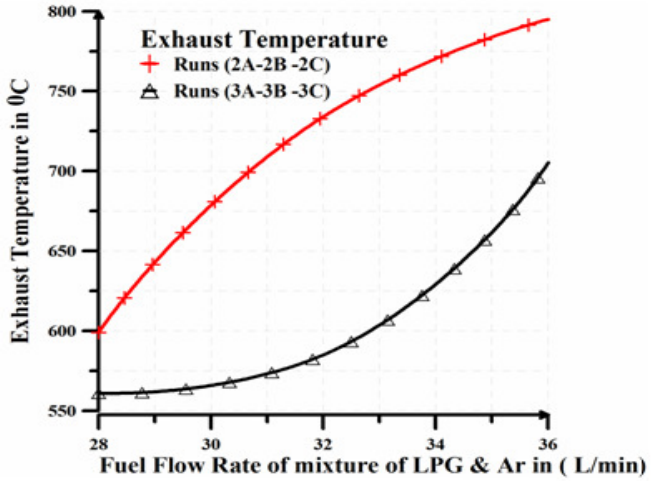

Panel a: variation of exhaust temperature with the flow rate of a mixture LPG and Argon.

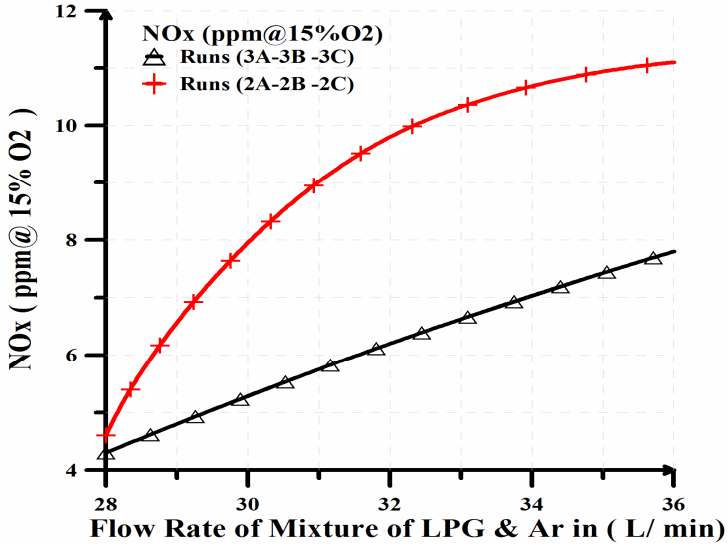

Panel b: variation of NOx emissions with the flow rate of a mixture LPG and Argon.

Fig. 16 . Panels a, b variation of exhaust temperature and NOx with input volume flow rate of mixture LPG and Argon.

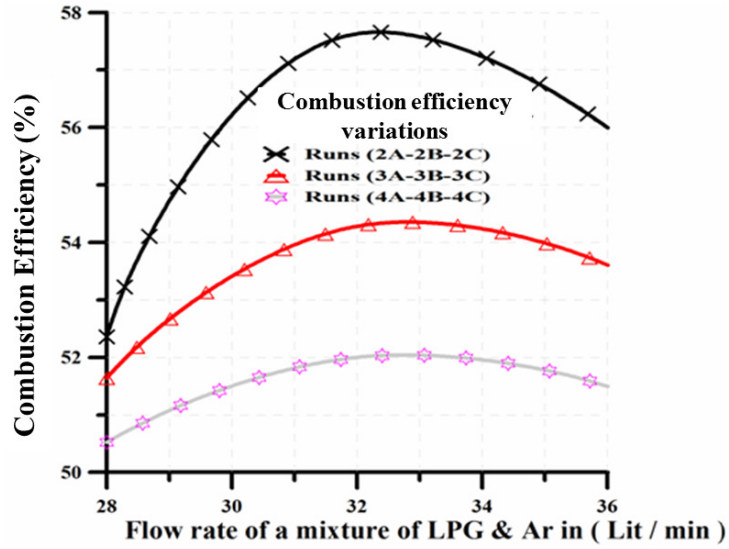

Fig. 17. Variation of combustion efficiency with input volume flow rate of mixture of LPG and Argon at different percentages runs (2A to 2C, 3A to 3C, 4A to 4C).

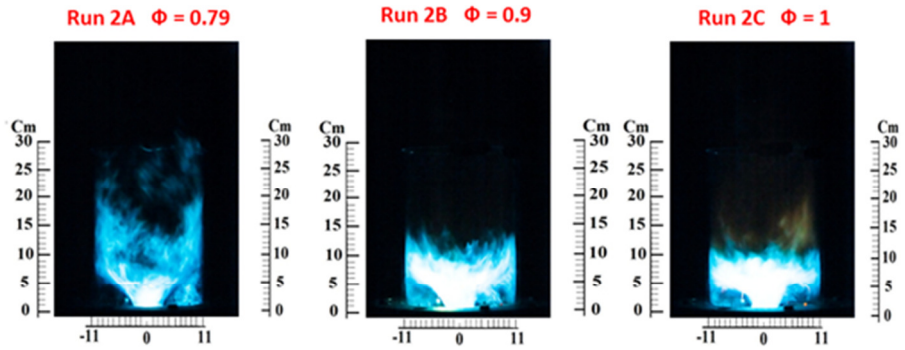

Panel a (Mixture 90% LPG with 10% Ar);[Runs 2A to2C].

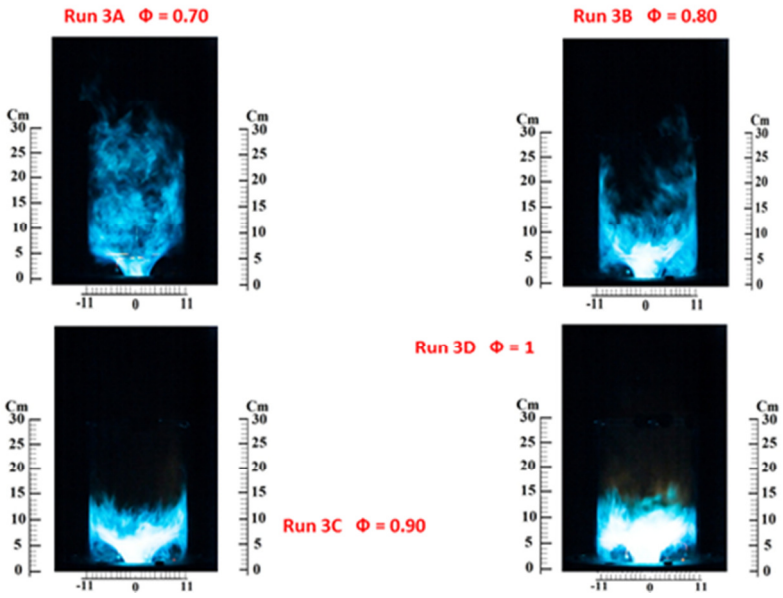

Panel b (Mixture 80%LPG with 20%Ar); [Runs 3Ato 3D].

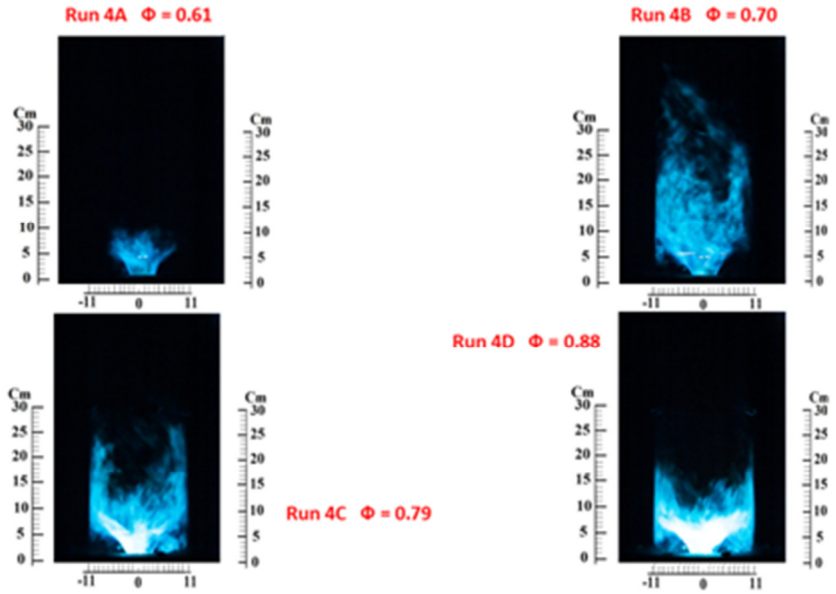

Panel c (Mixture 70%LPG with 30% Ar); [Runs 4A to 4D].

Fig. 18. Panels a, b, c visual images of LPG with argon diluents turbulent lean premixed flames at. (10 – 20 -30 % Argon) addition.

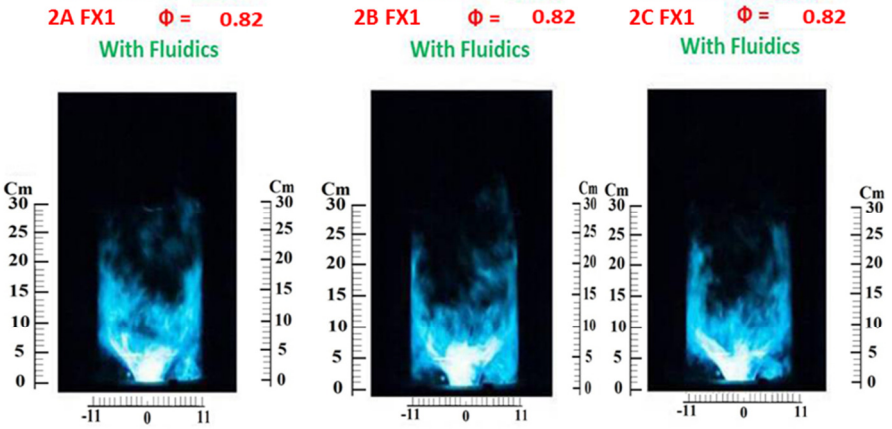

Panel a (Mixture of LPG with 10, 20, 30% Argon) with Fluidics ; [Cases 2A,2B,3C] FX1.

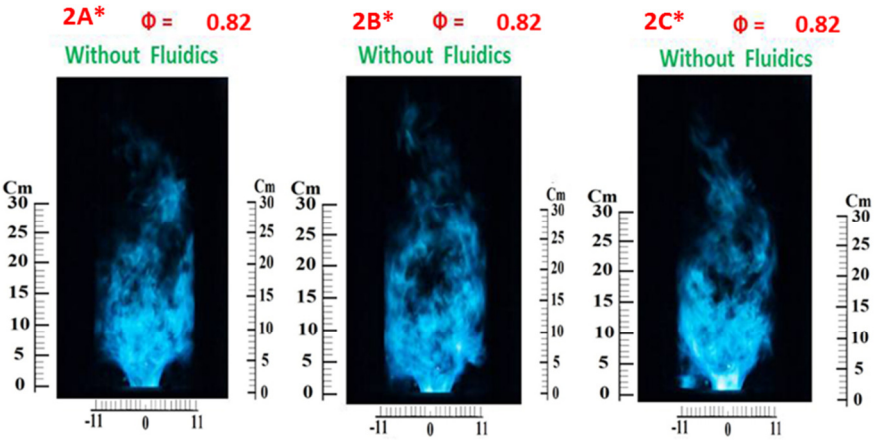

Fig. 19 . Visual images of mixtures LPG at fixed flow rate 26 Lit /min with (10-20-30 %) Argon diluents turbulent lean premixed flames ; Cases [2A- 3A- 4A with fluidics and 2A*- 2B*- 2C* without fluidics].

Table 1. Experimental program and measured quantities.

Experimental program					Measured quantities			
Case No.	Air flow rate L/min	LPG flow rate L/min	Ar flow rate L/min	Total mixture flow rate L/min	Φ	NOx ppm	℃ T_{exh}	η_{Comb} %
1	873	26	nil	26	0.82	6.45	652	55.93
2		32	nil	32	1	14.75	792	56.14
1FX1		26	nil	26	0.82	3.5	681	58.51
2FX1		32	nil	32	1	7.5	805	57.09
2A		25.2	2.8	28	٠,79	4.6	599	52.36
2B		28.8	3.2	32	٠,9	9.8	734	57.63
2C		32.4	3.6	36	1	11.1	795	56
3A		22.4	5.6	28	٠,7	4.3	561	55.64
3B		25.6	6.4	32	٠,8	6.2	585	51.28
3C		28.8	7.2	36	٠,9	7.8	705	55.61
3D		32	8	40	1	-	752	53.85
4A		19.6	8.4	28	0.61	-	451	50.52
4B		22.4	9.6	32	0.7	-	521	51.80
4C		25.2	10.8	36	0.79	8.4	570	50.91
4D		28	12	40	0.88	-	685	55.84
2A FX1		26	2.6	28.6	0.82	2.3	625	53.73
3A FX1		26	5.2	31.2	0.82	3.1	607	52.32
4A FX1		26	7.8	33.8	0.82	4.7	602	52.08